

SOLID-STATE COMPOUNDS OF 2-CHLOROBENZYLIDENE PYRUVATE WITH SOME BIVALENT METAL IONS

Synthesis, characterization and thermal behaviour

G. Bannach, A. B. Siqueira, E. Y. Ionashiro, E. C. Rodrigues and M. Ionashiro*

Instituto de Química, UNESP, CP 355, CEP 14801-970 Araraquara, SP, Brazil

Solid-state $M\text{-}2\text{-Cl-BP}$, where M stands for Mn, Fe, Co, Ni, Cu, Zn and Pb and 2-Cl-BP is 2-chlorobenzylidene pyruvate, have been synthesized. Thermogravimetry and derivative thermogravimetry (TG/DTG), simultaneous thermogravimetry and differential thermal analysis (TG-DTA), X-ray powder diffractometry, infrared spectroscopy, elemental analysis, and complexometry were used to characterize and to study the thermal behaviour of these compounds. The results led to information about the composition, dehydration, thermal stability and thermal decomposition of the isolated compounds.

Keywords: bivalent metals, 2-chlorobenzylidene pyruvate, coordination sites, thermal behaviour

Introduction

Synthesis of benzylidene pyruvic acid (HBP), as well as of phenyl-substituted derivatives of HBP, have been reported [1, 2]. These acids are of continuing interest as intermediates in pharmacological, industrial and chemical synthesis, in the development of enzymes, and in other ways [2–7].

Several metal ion complexes of phenyl-substituted derivatives of benzylidene pyruvate, $C_6H_5\text{-CH=CH-COCOO}^-$ (BP), have been investigated in aqueous solutions [8, 9] and in the solid-state [10–15]. In aqueous solutions these works reported the thermodynamic stability (β_1), and spectroscopic parameters ($\varepsilon_{1\max}$, λ_{\max}), associated with 1:1 complex species, as well as analytical applications of sodium 4-dimethylamino-BP for gravimetric determination of Cu(II), or as indicator in the complexometric titrations of Th(IV) and Al(III), with EDTA. In the solid state, the works reported the synthesis and investigation of the compounds by means of thermogravimetry and derivative thermogravimetry (TG/DTG), differential thermal analysis (DTA), X-ray powder diffractometry, and complexometry. Establishment of stoichiometry detailed knowledge of the thermal behaviour of the ligands and their metal ion compounds have been the main purposes of these studies.

In this paper, solid state compounds of bivalent manganese, iron, cobalt, nickel, copper, zinc and lead with 2-Cl-BP were prepared. The compounds were investigated by complexometry, elemental analysis, X-ray powder diffractometry, infrared spectroscopy, simultaneous thermogravimetry and differential ther-

mal analysis (TG-DTA) and differential scanning calorimetry (DSC). The data provided information concerning the thermal stability and thermal decomposition of these compounds in the solid-state.

Experimental

Sodium 2-chlorobenzylidene pyruvate and its corresponding acid were synthesized and purified, following the procedure described in the literature [15]. Aqueous solutions of the bivalent metal ions were prepared by dissolving the corresponding chlorides, except for lead, where the nitrate was used.

The solid compounds were prepared by adding slowly, with continuous stirring solutions, the ligand solution to the respective metal ion solutions until complete precipitation of the metal compounds. To avoid oxidation of Mn(II) and Fe(II), all their solutions as well as the water employed for washing their precipitates were employed for washing their precipitates were purged with nitrogen gas. The precipitates were washed until chloride (or nitrate) ions were eliminated, filtered through and dried on Whatman n° 42 filter paper and kept in a desiccator over anhydrous calcium chloride, under reduced pressure (10^3 Pa), to constant mass.

In the solid-state compounds, metal ions, water and 2-Cl-BP contents were determined from the TG curves. The metal ions were also determined by complexometry with standard EDTA solution [16, 17] after igniting the compounds to the respective oxides and their dissolution in hydrochloric or nitric acid.

* Author for correspondence: massaoi@iq.unesp.br

Carbon and hydrogen contents were determined by microanalytical procedures, with an EA 1110 CHNS-O Elemental Analyzer from CE Instruments.

X-ray powder patterns were obtained with a Siemens D-5000 X-ray diffractometer, using CuK α radiation ($\lambda=1.544 \text{ \AA}$) and setting of 40 kV and 20 mA.

Infrared spectra for 2-Cl-BP (sodium salt) as well as for its metal ions compounds, were run on a Nicolet model Impact 400 FTIR instruments, within 4000–400 cm^{-1} range. The solid samples were pressed into KBr pellets.

Simultaneous TG-DTA curves were obtained with thermal analysis system, model SDT 2960 from TA instruments. The purge gas was an air with flow of 150 mL min^{-1} . A heating rate of 10 K min^{-1} was adopted, with samples weighing about 7 mg. Alumina crucibles was used for TG-DTA.

Results and discussion

The analytical and thermoanalytical (TG) results of the synthesized compounds are shown in Table 1. These results permitted to establish the stoichiometry of the compounds, which are in agreement with general formula $M(2\text{-Cl-BP})_2 \cdot n\text{H}_2\text{O}$, where M represents Mn(II), Fe(II), Co(II), Ni(II), Cu(II), Zn(II) and Pb(II), 2-Cl-BP is 2-chlorobenzylideneypyruvate and $n=0.5(\text{Pb})$, 1.5(Zn), 2(Mn, Co, Cu), 2.5(Ni) or 3(Fe).

The X-ray powder patterns (Fig. 1) show that the manganese, iron, copper and lead compounds have a crystalline structure, without evidence of the formation of isomorphous compounds, and that the cobalt, nickel and zinc compounds are amorphous.

Infrared spectroscopic data of complexes of 2-chlorobenzylideneypyruvate (sodium salt) with metal ions considered in this work are shown in Table 2. The investigation was focused mainly within the 1700–1400 cm^{-1} range because this region is potentially most informative in attempting to assign coordination sites.

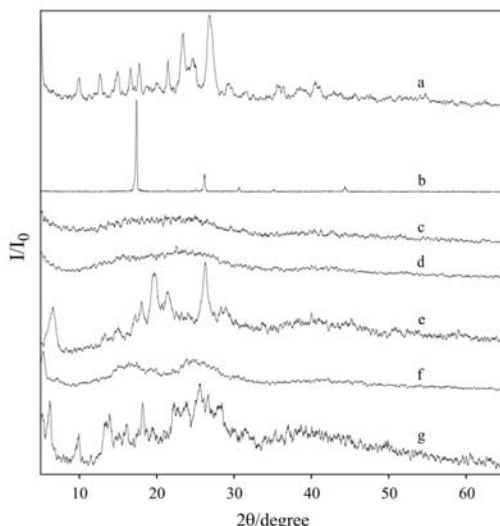


Fig. 1 X-ray powder diffraction patterns of the compounds:
a – $\text{Mn}(\text{L})_2 \cdot 2\text{H}_2\text{O}$; b – $\text{Fe}(\text{L})_2 \cdot 3\text{H}_2\text{O}$, c – $\text{Co}(\text{L})_2 \cdot 2\text{H}_2\text{O}$,
d – $\text{Ni}(\text{L})_2 \cdot 2.5\text{H}_2\text{O}$, e – $\text{Cu}(\text{L})_2 \cdot 2\text{H}_2\text{O}$, f – $\text{ZnL}_2 \cdot 1.5\text{H}_2\text{O}$
and g – $\text{Pb}(\text{L})_2 \cdot 0.5\text{H}_2\text{O}$

In 2-Cl-BP (sodium salt), strong band at 1616 cm^{-1} and a medium intensity band located at 1404 cm^{-1} are attributed to the anti-symmetrical and symmetrical frequencies of the carboxylate groups, respectively [18, 19]. The band centered at 1684 cm^{-1} is typical of a conjugated ketonic carbonyl group [18–20].

The band assigned to the anti-symmetrical stretching carboxylate frequencies as well as that assigned to the carbonyl are shifted to lower values relatives to the corresponding frequencies in 2-Cl-BP itself (sodium salt). This behaviour indicates that both groups act as coordination centers in the metal compounds [20, 21]. The data displayed in Table 2 show that the magnitude of the shifts are dependent on the metal ions, and are in agreement with the same bivalent metals and lanthanides with other phenyl substituted derivatives of BP [11–13].

Simultaneous TG-DTA and TG, DTG curves are shown in Fig. 2. The TG-DTA curves show mass losses in three our four steps, corresponding to endo-

Table 1 Analytical, thermoanalytical (TG) and elemental analysis data of the compounds, $\text{ML}_2 \cdot n\text{H}_2\text{O}$

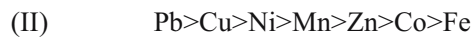
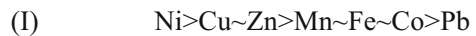
Compounds	Metal/%			L loss/%		Water/%		Carbon/%		Hydrogen/%		Residue ^a
	Calcd	EDTA	TG	Calcd	TG	Calcd	TG	Calcd	EA	Calcd	EA	
$\text{Mn}(\text{L})_2 \cdot 2\text{H}_2\text{O}$	10.77	10.59	11.17	77.99	77.32	7.06	7.18	47.08	46.95	3.16	3.92	Mn_3O_4
$\text{Fe}(\text{L})_2 \cdot 3\text{H}_2\text{O}$	10.48	10.80	10.56	74.19	74.09	10.82	10.81	45.40	45.64	3.43	4.18	Fe_2O_3
$\text{Co}(\text{L})_2 \cdot 2\text{H}_2\text{O}$	11.46	11.28	11.04	77.38	78.11	7.01	6.85	46.72	46.01	3.14	3.67	Co_3O_4
$\text{Ni}(\text{L})_2 \cdot 2.5\text{H}_2\text{O}$	11.22	11.18	10.91	77.10	77.48	8.62	8.63	45.93	45.35	3.28	3.11	NiO
$\text{Cu}(\text{L})_2 \cdot 2\text{H}_2\text{O}$	12.25	12.11	—	77.72	89.58	6.95	7.05	46.30	46.05	3.11	3.89	CuO
$\text{Zn}(\text{L})_2 \cdot 1.5\text{H}_2\text{O}$	12.78	12.31	—	78.81	84.86	5.28	4.73	46.95	45.24	2.96	3.34	ZnO
$\text{Pb}(\text{L})_2 \cdot 0.5\text{H}_2\text{O}$	32.61	32.65	—	63.46	92.85	1.42	1.81	37.80	37.60	2.07	3.02	PbO

L – 2-chlorobenzylideneypyruvate; ^aall the residues was confirmed by X-ray powder diffractometry

thermic peaks due to dehydration and exothermic peaks attributed to the oxidation of organic matter, in spite of the DTG curves to show that the thermal decomposition occurs with a large number of consecutive and/or overlapping steps and through a more complex pathway than that observed from TG curves.

The thermal stability of the anhydrous compounds (I), as well as the final temperature of thermal decomposition (II) as shown by the TG-DTA and

DTG curves, depends on the nature of the metal ion, and they follow the order:



As, can be seen in Table 3.

The thermal behaviour of the compounds is heavily dependent on the nature of the metal ion and so the features of each of these compounds are discussed individually as follows:

Table 2 Infrared spectroscopic data of 2-chlorobenzylidene pyruvate and its compounds with the metal ions

Compounds	$\nu_{(O-H)}$	ν_{H_2O}	$\nu_{as(COO^-)}$	$\nu_{as(COO^-)}$	$\nu_{(C=O)}$
NaL·1.5H ₂ O		3446 m	1404 m	1616 s	1684 s
Mn(L) ₂ ·2H ₂ O		3396 m	1427 m	1595 s	1664 w
Fe(L) ₂ ·3H ₂ O		3470 m	1414 m	1595 s	1676 w
Co(L) ₂ ·2H ₂ O		3373 m	1427 m	1585 s	1641 s
Ni(L) ₂ ·2.5H ₂ O		3394 m	1431 m	1583 s	1639 s
Cu(L) ₂ ·2H ₂ O		3385 m	1400 m	1605 s	1660 s
Zn(L) ₂ ·1.5H ₂ O		3402 m	1431 m	1589 s	1645 s
Pb(L) ₂ ·0.5H ₂ O		3431 m	1339 w	1593 s	1660 w

L – 2-chlorobenzylidene pyruvate; s – strong; m – medium; w – weak; $\nu_{as(O-H)}$ – hydroxyl group stretching frequency; $\nu_{as(COO^-)}$ and $\nu_{as(COO^-)}$ – symmetrical and anti-symmetrical vibrations of the COO⁻ group; $\nu_{(C=O)}$ – carbonyl stretching vibration frequency

Table 3 Temperature ranges, mass losses and peak temperature observed for each step of the TG-DTA curves of the compounds

Compounds		Step					
		first	second	third	fourth	fifth	sixth
Mn(L) ₂ ·2H ₂ O	θ/K	323–413	413–743	743–853			
	Loss/%	7.18	44.45	33.87			
	Peak/K	398(endo)	553(exo)	793(exo)			
Fe(L) ₂ ·3H ₂ O	θ/K	343–403	413–603	603–673	673–833		
	Loss/%	10.36	24.58	15.28	34.83		
	Peak/K	398(endo)	483(exo)	633(exo)	813(exo)		
Co(L) ₂ ·2H ₂ O	θ/K	323–413	413–593	593–673	673–793	793–838	1173–1198
	Loss/%	6.85	19.94	13.96	32.58	10.56	1.07
	Peak/K	373(endo)	558(exo)	613(exo)	783(exo)	828(exo)	1188(endo)
Ni(L) ₂ ·2.5H ₂ O	θ/K	323–448	448–713	713–880			
	Loss/%	8.63	50.20	27.06			
	Peak/K	378(endo)	598, 663(exo)	798, 843(exo)			
Cu(L) ₂ ·2H ₂ O	θ/K	323–413	423–508	508–603	603–893		
	Loss/%	7.05	14.06	20.17	48.29		
	Peak/K	403(endo)	483(exo)	573(exo)	798(exo)		
Zn(L) ₂ ·1.5H ₂ O	θ/K	323–403	423–513	513–683	683–848		
	Loss/%	4.73	4.66	35.29	44.62		
	Peak/K	378(endo)	513 (exo)	603 (exo)	803 (exo)		
Pb(L) ₂ ·0.5H ₂ O	θ/K	323–393	413–593	593–723	723–943		
	Loss/%	1.81	15.32	11.62	65.91		
	Peak/K	363(endo)	523(exo)	628(exo)	813, 893(exo)		

L – 2-chlorobenzylidene pyruvate

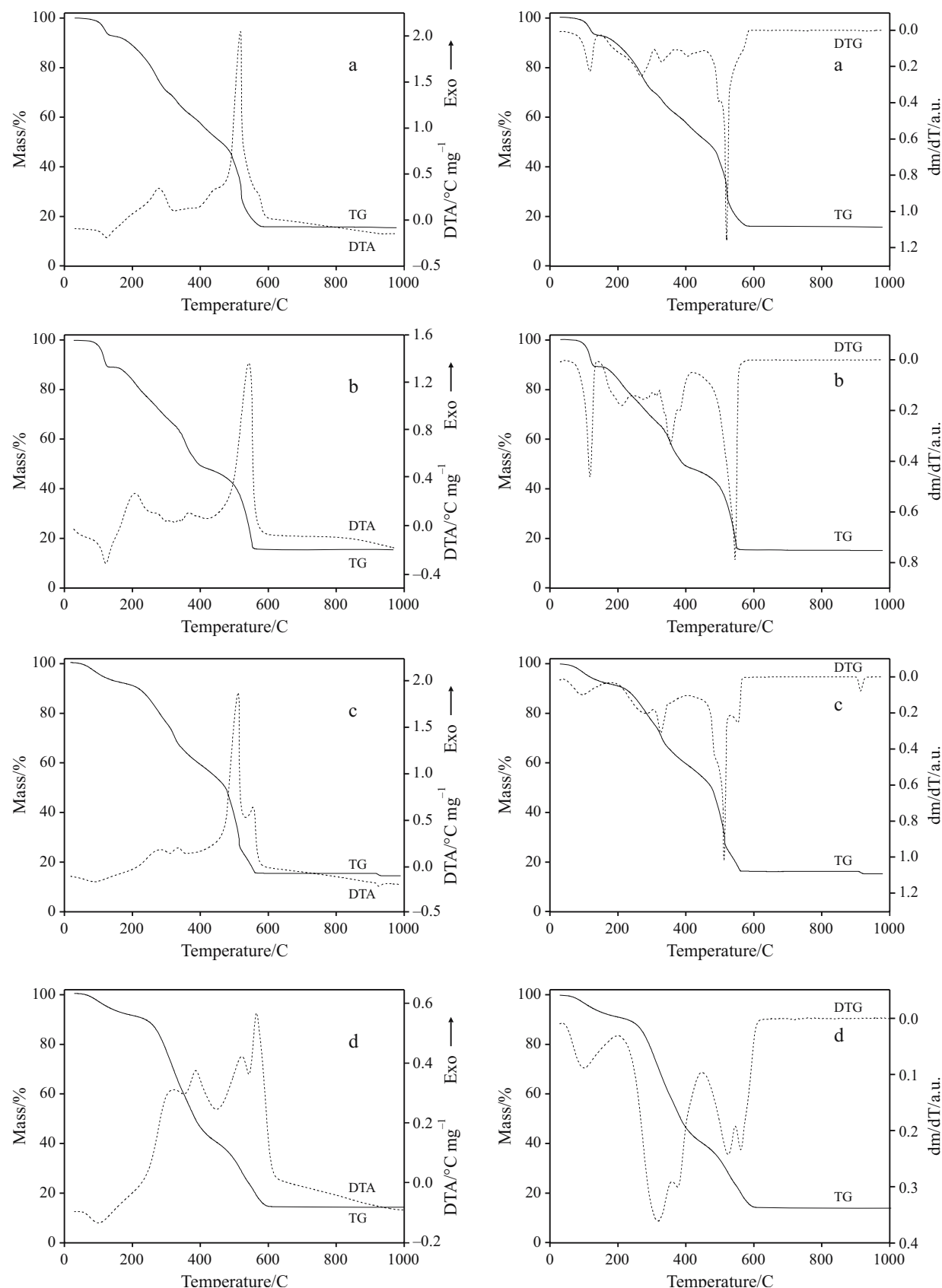


Fig. 2 TG-DTA and TG/DTG curves of 2-chlorobenzylidene pyruvate and its compounds with: a – Mn ($m=7.173$ mg), b – Fe ($m=6.980$ mg), c – Co ($m=6.990$ mg), d – Ni ($m=6918$ mg)

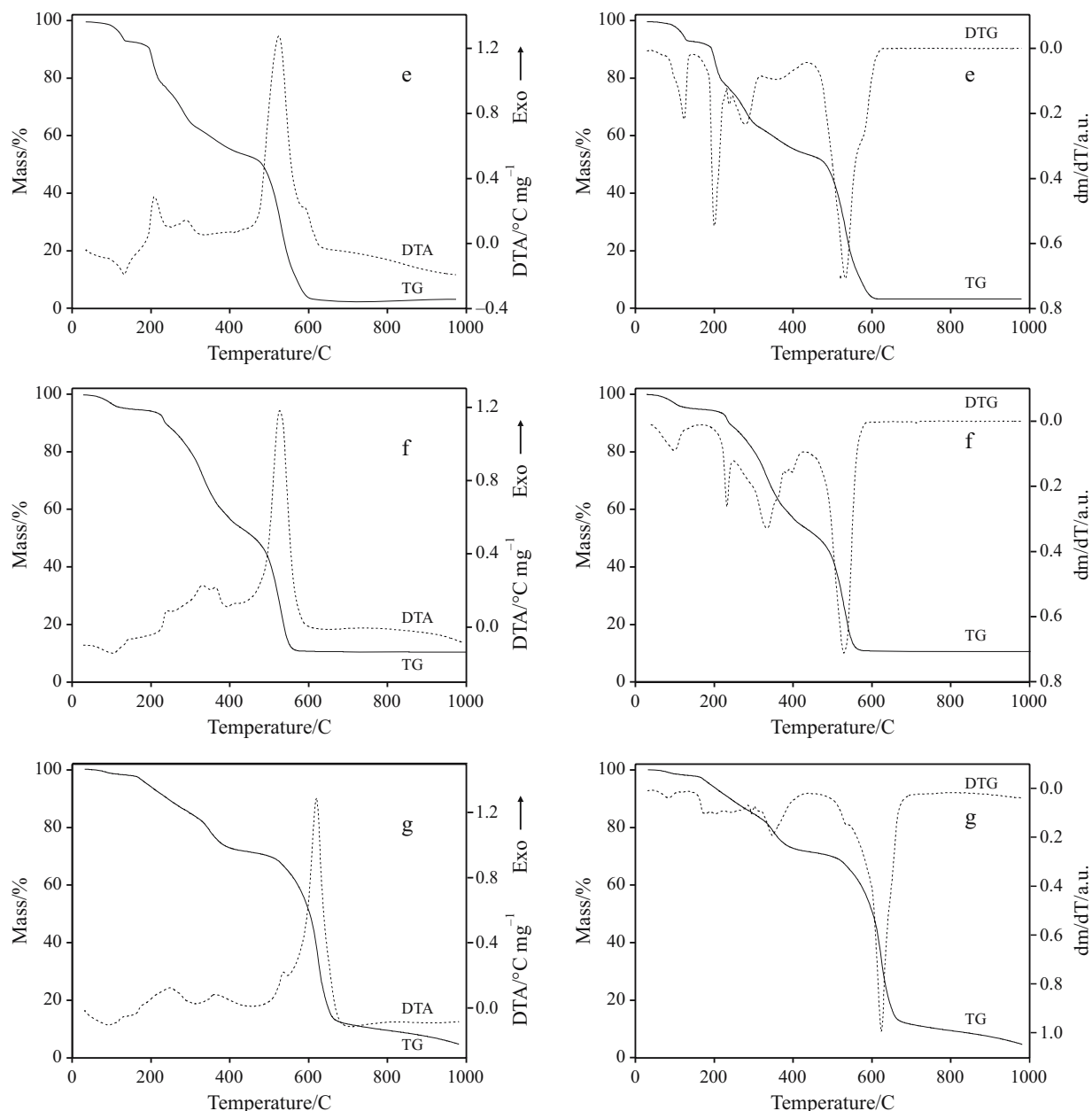


Fig. 2 TG-DTA and TG/DTG curves of 2-chlorobenzylidene pyruvate and its compounds with: e – Cu ($m=7.007$ mg), f – Zn ($m=6.947$ mg), g – Pb ($m=6.921$ mg)

Manganese compound

The simultaneous TG-DTA and TG, DTG curves are shown in Fig. 2a. The first mass loss that occurs between 323 and 413 K, corresponding to an endothermic peak at 398 K is due to dehydration with loss of $2\text{H}_2\text{O}$ (Calcd.=7.06%, TG=7.18%). The thermal decomposition of the anhydrous compound, the DTG curve shows mass loss in four steps, however the TG curve suggests two overlapping steps: between 413–743 and 743–853 K with losses of 43.45 and 33.87%, respectively, corresponding to the exothermic peak at 553 and 793 K, which are attributed to ox-

idation of the organic matter. The total mass loss up to 853 K is in agreement with the formation of Mn_3O_4 as final residue (Calcd.=85.05%; TG=84.50%) and confirmed by X-ray powder diffractometry.

Iron compound

The simultaneous TG-DTA and TG, DTG curves are shown in Fig. 2b. The first mass loss observed between 343–403 K corresponding to an endothermic peak at 398 K is to the dehydration with loss of $3\text{H}_2\text{O}$ (Calcd.=10.22%; TG=10.36%). The thermal decomposition of the anhydrous compound the DTG curve

suggest four consecutive and/or overlapping steps. On the contrary, the TG curve shows only three steps, the first two being overlapping ones between 413–603, 603–673 K causing 24.3 and 15.3% mass losses. The third one in the 673–833 K temperature range shows 34.8% mass change. The corresponding exothermic peak temperature are 483, 633 and 813 K are due to the oxidation of Fe(II) to Fe(II) and of the organic matter. The total mass loss up to 833 K is in agreement with the formation of Fe_2O_3 as final residue (Calcd.=84.91%; TG=84.74%) which was confirmed by X-ray powder diffractometry.

Cobalt compound

The simultaneous TG-DTA and TG, DTG curves are shown in Fig. 2c. The first mass loss that occurs between 323 and 413 K, corresponding to an endothermic peak at 373 K is due to dehydration with loss of $2\text{H}_2\text{O}$ (Calcd.=7.01%; TG=6.85%). The thermal decomposition of the anhydrous compound, the TG-DTA and DTG curves show mass losses in four overlapping steps: between 413–593, 593–673, 673–793 and 793–838 K, with losses of 19.94, 13.96, 32.58 and 10.56% respectively, corresponding to exothermic peaks at 558, 613, 783 and 838 K, attributed to oxidation of the organic matter. The total mass loss up to 838 K is in agreement with the formation of Co_3O_4 (Calcd.=84.39%; TG=83.89%). The last mass loss that occurs between 1173 and 1198 K, corresponding to the endothermic peak at 1188 K is due to reduction of Co_3O_4 to CoO (Calcd.=1.04%; TG=1.07%), in agreement with literature [10, 22, 23]. The X-ray powder pattern of the residue obtained at 1223 K, is coincident with that obtained for Co_3O_4 , this is due to the reoxidation reaction of CoO to Co_3O_4 which occurs on cooling the former in an air atmosphere at room temperature [22, 23].

Nickel compound

The TG-DTA and TG, DTG curves are shown in Fig. 2d. The first mass loss that occurs between 323 and 448 K corresponding to an endothermic peak at 378 K is due to dehydration with loss of $2.5\text{H}_2\text{O}$ (Calcd.=8.62%; TG=8.63%). The thermal decomposition of the anhydrous compound the DTG and DTA shows mass losses in four consecutive and/or overlapping steps, nevertheless the TG curve suggests two steps: between 448–713 and 713–880 K, with loss of 50.20 and 27.06%, respectively, corresponding to exothermic peaks at 598, 663, 798 and 843 K, attributed to oxidation of the organic matter. The total mass loss up to 880 K, is in agreement with the formation of NiO as final residue (Calcd.=85.72%; TG=86.11%) and confirmed by X-ray powder diffractometry.

Copper compound

The TG-DTA and TG, DTG curves are shown in Fig. 2e. The mass loss observed between 323 and 413 K, corresponding to an endothermic peak at 403 K is due to dehydration with loss of $2\text{H}_2\text{O}$ (Calcd.=6.95%; TG=7.05%). The thermal decomposition of the anhydrous compound, the DTG suggest four consecutive and/or overlapping steps, however the TG curves show three steps: between 423–508, 508–603 and 603–893 K with mass losses of 14.06, 20.17 and 48.29%, respectively. The mass losses corresponds to exothermic peaks at 483, 573 and 798 K. The total mass loss up to 893 K is in disagreement with the formation of CuO as final residue (Calcd.=84.67%, TG=89.57%), nevertheless the formation of CuO was confirmed by X-ray powder diffractometry.

Zinc compound

The TG-DTA and TG, DTG curves are shown in Fig. 2f. The mass loss that occurs between 323 and 403 K, corresponding to an endothermic peak at 378 K is due to dehydration with mass loss of $1.5\text{H}_2\text{O}$ (Calcd.=5.28%; TG=4.73%). Thermal decomposition of the anhydrous compound, the TG-DTA and DTG curve show mass losses in three overlapping steps: between 423–513, 513–683 and 683–848 K with losses of 4.66, 3529 and 44.62%, respectively, corresponding to exothermic peaks at 513, 603 and 803 K, attributed to oxidation of organic matter. The total mass loss up to 848 K is in disagreement with the formation of ZnO as final residue. (Calcd.=84.09%, TG=89.30%) however the X-ray powder diffractometry confined the formation of ZnO .

Lead compound

The TG-DTA and TG, DTG curves are shown in Fig. 2g. The first mass loss that occurs between 323 and 393 K corresponding to an endothermic peak at 363 K is due to dehydration with loss of $0.5\text{H}_2\text{O}$ (Calcd.=1.42%; TG=1.81%). The thermal decomposition of the anhydrous compound, the TG-DTA and DTG curves show mass losses in three steps: between 413–593, 593–723 and 723–943 K with losses of 15.32, 11.62 and 65.91%, respectively, corresponding to exothermic peaks at 523, 628, 813 and 893 K, attributed to oxidation of the organic matter. The total mass loss up to 943 K is in disagreement with the formation of PbO as final residue. (Calcd.=64.88%, TG=94.66%) however the X-ray powder diffractometry confined the formation of PbO .

In the copper, zinc and lead compounds, the total mass loss is in disagreement with TG results, due to the partial volatilization of these metals which was

confirmed by qualitative test on the evolved gas collected in the purge gas outlet of the thermobalance. The volatilization of these metals probably occurs as chloride, suggesting reaction of chloro of the ligand with these metal ions during the thermal decomposition.

Conclusions

From TG curves, complexometry and elemental analysis data, a general formula could be established for the synthesized compounds. The X-ray powder patterns pointed out that the manganese, iron, copper and lead compounds have a crystalline structure, without evidence concerning the formation of isomorphous compounds, and that the cobalt, nickel and zinc compounds were obtained in the amorphous state. The infrared spectroscopy data suggest that 2-Cl-BP anion acts as a bidentate ligand towards the metal ions considered in this work.

The TG-DTA curves provided previously unreported information concerning the thermal behaviour and thermal decomposition of these compounds.

Acknowledgements

The authors thank FAPESP and CNPq Foundations (Brazil) for financial support.

References

- 1 E. D. Stecher, M. J. Incovia, B. Kerben, D. Lavine, M. Oen and E. Suhl, *J. Org. Chem.*, 38 (1973) 4453 and references therein.
- 2 A. J. L. Cooper, J. Z. Ginos and A. Meister, *Chem. Rev.*, 83 (1981) 321.
- 3 A. K. Datta and T. C. Daniels, *J. Pharm. Sci.*, 52 (1963) 905.
- 4 W. Mayer, H. Rudolph and E. De Cleur, *Angew. Makromol. Chem.*, 93 (1981) 83.
- 5 A. I. Baba, W. Eang, W. Y. Kim, L. Strong and R. H. Schmehl, *Synth. Commun.*, 24 (1994) 1029.
- 6 G. Dujardim, M. Mandet and E. Brown, *Tetrahedron Lett.*, 38 (1997) 1555.
- 7 G. Dujardim, S. Leconte, A. Bernard and E. Brown, *Synlett*, (2001) 147.
- 8 C. B. Melios, V. R. Torres, M. H. A. Mota, J. O. Tognolli and M. Molina, *Analyst*, 109 (1984) 385.
- 9 R. N. Marques, C. B. Melios, N. C. S. Pereira, O. S. Siqueira, M. Moraes, M. Molina and M. Ionashiro, *J. Alloys Compd.*, 249 (1997) 102 and references therein.
- 10 R. A. Mendes, M. A. S. Carvalho Filho, N. S. Fernandes, L. M. D'Assunção, C. B. Melios and M. Ionashiro, *An. Assoc. Brás. Quím.*, 47 (1998) 329.
- 11 I. A. Petroni, F. L. Fertonani, C. B. Melios and M. Ionashiro, *Thermochim. Acta*, 400 (2003) 187 and references therein.
- 12 N. S. Fernandes, M. A. S. Carvalho Filho, C. B. Melios and M. Ionashiro, *J. Therm. Anal. Cal.*, 73 (2003) 307.
- 13 N. S. Fernandes, M. A. S. Carvalho Filho, R. A. Mendes, C. B. Melios and M. Ionashiro, *J. Therm. Anal. Cal.*, 76 (2004) 193.
- 14 E. Y. Ionashiro, F. L. Fertonani, C. B. Melios and M. Ionashiro, *J. Therm. Anal. Cal.*, 79 (2005) 299.
- 15 G. Bannach, R. A. Mendes, E. Y. Ionashiro, A. E. Mauro, E. Schnitzler and M. Ionashiro, *J. Therm. Anal. Cal.*, 79 (2005) 329.
- 16 H. A. Flaschka, *EDTA Titrations*, Pergamon Press, Oxford 1964.
- 17 C. N. de Oliveira, M. Ionashiro and C. A. F. Graner, *Ecl. Quím.*, 10 (1985) 7.
- 18 G. Sócrates, *Infrared Characteristic Group Frequencies*, 2nd Ed., Wiley, New York 1994, pp. 91, 236–237.
- 19 R. M. Silverstein and F. X. Webster, *Spectrometric Identifications of Organic Compounds*, 6th Ed., Wiley, New York 1998, pp. 92, 93, 96 and 97.
- 20 F. A. Cotton, *The Infrared Spectra of Transition Metal Complexes in Modern Coordination Chemistry*, J. Lewis and R. G. Wilkins, Eds., Interscience, New York 1960, pp. 397–386.
- 21 K. Nakamoto, *Infrared and Raman Spectra of Inorganic and Coordination Compounds*, Part B, 5th Ed., Wiley, New York 1997, pp. 58–61.
- 22 G. A. El-Shobaky, A. S. Ahmad, A. N. Al Noaimi and H. G. El-Shobaky, *J. Thermal Anal.*, 46 (1996) 1801.
- 23 Z. P. Xu and H. C. Zeng, *J. Matter Chem.*, 8 (1998) 1499.

Received: December 19, 2005

Accepted: May 8, 2007

OnlineFirst: August 31, 2007

DOI: 10.1007/s10973-005-7060-6